1 FEBRUARY 2019 WANG ET AL. 843

Dynamics of Asian Summer Monsoon Response to Anthropogenic Aerosol Forcing

HAI WANG

Physical Oceanography Laboratory, Collaborative Innovation Center of Marine Science and Technology, Ocean University of China, and Qingdao National Laboratory for Marine Science and Technology, and College of Oceanic and Atmospheric Sciences, Ocean University of China, Qingdao, China

SHANG-PING XIE

Scripps Institution of Oceanography, University of California, San Diego, La Jolla, California, and Physical Oceanography Laboratory, Collaborative Innovation Center of Marine Science and Technology, Ocean University of China, and Qingdao National Laboratory for Marine Science and Technology, Oingdao, China

YU KOSAKA

Research Center for Advanced Science and Technology, University of Tokyo, Komaba, Meguro-ku, Tokyo, Japan

OINYU LIU

Physical Oceanography Laboratory/CIMST, Ocean University of China and Qingdao National Laboratory for Marine Science and Technology, and College of Oceanic and Atmospheric Sciences, Ocean University of China, Qingdao, China

YAN DU

State Key Laboratory of Tropical Oceanography, South China Sea Institute of Oceanology, Chinese Academy of Sciences, Guangzhou, China

(Manuscript received 19 June 2018, in final form 27 November 2018)

ABSTRACT

Anthropogenic aerosols partially mask the greenhouse warming and cause the reduction in Asian summer monsoon precipitation and circulation. By decomposing the atmospheric change into the direct atmospheric response to radiative forcing and sea surface temperature (SST)-mediated change, the physical mechanisms for anthropogenic-aerosol-induced changes in the East Asian summer monsoon (EASM) and South Asian summer monsoon (SASM) are diagnosed. Using coupled and atmospheric general circulation models, this study shows that the aerosol-induced troposphere cooling over Asian land regions generates anomalous sinking motion between 20° and 40°N and weakens the EASM north of 20°N without SST change. The decreased EASM precipitation and the attendant wind changes are largely due to this direct atmospheric response to radiative forcing, although the aerosol-induced North Pacific SST cooling also contributes. The SST-mediated change dominates the aerosol-induced SASM response, with contributions from both the north-south interhemispheric SST gradient and the local SST cooling pattern over the tropical Indian Ocean. Specifically, with large meridional gradient, the zonal-mean SST cooling pattern is most important for the Asian summer monsoon response to anthropogenic aerosol forcing, resulting in a reorganization of the regional meridional atmospheric overturning circulation. While uncertainty in aerosol radiative forcing has been emphasized in the literature, our results show that the intermodel spread is as large in the SST effect on summer monsoon rainfall, calling for more research into the ocean-atmosphere coupling.

Corresponding author: Hai Wang, wanghai@ouc.edu.cn

1. Introduction

Dramatic increase in anthropogenic aerosol emissions has caused pronounced climate change since the industrial revolution (Kaufman et al. 2002; Bao et al. 2009; Lamarque et al. 2010; Donner et al. 2011 Boucher et al. 2013). While the global mean radiative forcing is smaller than that of greenhouse gases (GHGs), aerosols can induce strong large-scale atmospheric circulation change and regional climate responses (Ming and Ramaswamy, 2011; Xie et al. 2013; Wang et al. 2016a) because of strong spatial distribution. The southward shift of the intertropical convergence zone (ITCZ) during the latter half of the twentieth century (Hwang et al. 2013; Allen et al. 2015; Wang et al. 2016b), the Sahel drought during the 1950s-1980s (Held et al. 2005; Chang et al. 2011; Booth et al. 2012; Dong and Sutton 2015), and the weakened Asian summer monsoon during the latter half of the twentieth century (Bollasina et al. 2011; Ganguly et al. 2012a,b; Song et al. 2014; Li et al. 2015; Li et al. 2016; Singh, 2016; Lau and Kim 2017; Li et al. 2018) are examples.

The East Asian summer monsoon (EASM) and the South Asian summer monsoon (SASM) provide about 70%–80% of the annual-mean precipitation for much of China and India (Gong and Wang 2000; Zhai et al. 2005; Piao et al. 2010). The Asian summer monsoon has shown considerable changes under anthropogenic aerosol forcing, with tremendous impacts on water resources, agriculture, economies, and ecosystem (Ma et al. 2017). Understanding the dynamical mechanism of Asian summer monsoon response to changing radiative forcing has important societal implications.

The potential impacts of anthropogenic aerosols on the Asian summer monsoon have drawn much attention in recent years (Li et al. 2016). Previous studies suggested both the local and nonlocal effects of anthropogenic aerosols on the EASM (Dong et al. 2016) and SASM (Bollasina et al. 2014) to weaken. Results from coupled climate models revealed that the weakened low-level EASM circulation and the drying trend over East Asia induced by anthropogenic aerosols dominated among the other external forcings during the second half of the twentieth century (Song et al. 2014). By decomposing the precipitation change in coupled climate models into thermodynamic and dynamic components via a moisture budget analysis, Li et al. (2015) concluded that atmospheric circulation change is key to the aerosol effect of drying East Asia. Over South Asia, Bollasina et al. (2011) attributed the observed precipitation decrease to anthropogenic aerosol forcing.

Although there is a general recognition that the anthropogenic aerosols weaken the Asian summer monsoon, the detailed mechanisms remain not fully understood. The aerosol-induced climate change may be decomposed into a direct atmospheric response

to radiative forcing without sea surface temperature (SST) change and an SST-mediated response (Shaw and Voigt 2015; Richardson et al. 2016). In the direct atmospheric response, aerosols affect precipitation and atmospheric circulation by modifying radiation and cloud physics (Menon et al. 2002; Lau et al. 2006; Rosenfeld et al. 2008; Bollasina et al. 2013). Besides, the carbonaceousaerosol-induced Tibetan Plateau snowpack pollution can also influence the Asian hydrological cycle and monsoon climate (Qian et al. 2011). The SST-mediated response refers to the atmospheric circulation change regulated by the anthropogenic-aerosol-induced SST change via coupled ocean–atmosphere interaction processes (Xie et al. 2013; Xu and Xie 2015; Wang et al. 2016a,b).

Using atmospheric general circulation model (AGCM) simulations, Ganguly et al. (2012b) separated the "fast and slow responses" (e.g., the direct atmospheric response and SST-mediated response) to aerosol forcing and concluded that the total precipitation change over South Asia resembles the slow response, whereas the fast component dominates land rainfall change north of 25°N. Recently, Li et al. (2018) analyzed the physical mechanisms of aerosol-induced Asian summer monsoon change and emphasized the importance of "fast atmospheric adjustments." Furthermore, they discussed a possible SST feedback via an idealized AGCM experiment but did not focus on the distinct response mechanisms between the EASM and SASM to anthropogenic aerosol forcing. What are the relative contributions of direct atmospheric response to aerosol forcing and SST feedback to the EASM and SASM changes? More importantly, though previous studies have confirmed the aerosol-induced SST effects on monsoonal precipitation, it is still unclear which aspects of the SST change are most important: the uniform cooling, the global meridional temperature gradient, or the regional SST pattern.

The present study extends previous studies of Asian summer monsoon response to anthropogenic aerosol forcing by identifying key differences between EASM and SASM in pattern and mechanism. By decomposing the climate response in the coupled historical anthropogenic-aerosol-only forcing experiment into direct atmospheric response and SST-mediated response, we diagnose the changes of EASM and SASM separately and examine relative contributions by the two components. Using a suite of idealized AGCM experiments, we evaluate the effects of the aerosol-induced uniform SST cooling, north–south interhemispheric asymmetry, and the regional SST cooling pattern in shaping the Asian summer monsoon changes.

The rest of the paper is organized as follows. Section 2 introduces the model simulations and the method that decomposes the coupled response into the direct atmospheric

TABLE 1. List of CMIP5 models used in this study.

Model acronym	Expansion
CanESM2	Second Generation Canadian Earth System Model
CSIRO Mk3.6.0	Commonwealth Scientific and Industrial Research Organisation Mark 3.6.0
GFDL CM3 ^a	Geophysical Fluid Dynamics Laboratory Climate Model, version 3
IPSL-CM5A-LR	L'Institut Pierre-Simon Laplace Coupled Model, version 5A, low resolution
NorESM1-M	Norwegian Earth System Model, version 1 (intermediate resolution)

^a The AOD data are from GFDL CM3.

and SST-mediated responses. Section 3 describes the direct adjustments of EASM and SASM in response to anthropogenic aerosol forcing. Section 4 reveals how the aerosol-induced SST feedbacks regulate the EASM and SASM changes. Section 5 investigates the relative contribution of direct atmospheric response and SST-mediated response in shaping the Asian summer monsoon response to anthropogenic aerosol forcing. The main conclusions are summarized and discussed in section 6.

2. Models and methods

This study focuses on the climate response to anthropogenic aerosol forcing. To reduce internal variability, we use a multimodel ensemble of five climate models from the phase 5 of the Coupled Model Intercomparison Project (CMIP5) archive (listed in Table 1; Taylor et al. 2012) that performed all the following experiments. 1) The historical anthropogenic aerosol single-forcing experiment (historical AA). In this experiment, the anthropogenic aerosols are the only time-varying forcing agent with the other forcing fixed at the preindustrial level. Details of the forcing agents used in the historical-AA simulations are described by Collins et al. (2013). The historical single-forcing simulations help us yield an estimation of the contribution of anthropogenic-aerosol-induced climate change from the preindustrial to 2000, including both direct atmospheric responses and SST-mediated changes R_{total} ; 2) The Hansen-style (Hansen et al. 2005) diagnostic experiments with atmospheric parts of the CMIP5 models listed in Table 1. The baseline for prescribed climatological SST experiments (sstClim) is an atmosphereonly run driven by prescribed SST and sea ice consistent with the climatology of the preindustrial control run $R_{\rm clim}$. The perturbed run for Hansen-style diagnosis of "fast" climate system responses to anthropogenic aerosols (sstClimAerosol) is designed to isolate the direct atmospheric changes with SST fixed at the

TABLE 2. AGCM experiments design.

Name	Prescribed SST
Control	SST _{clim}
SST_global	SST _{clim} + SSTA ^a (global)
SST_uniform	$SST_{clim} + (-0.51^{\circ}C)^{b}$
SST_global_zm	SST _{clim} + SSTA (global zonal mean)
SST_tropical_IO	SST _{clim} + SSTA (tropical Indian Ocean ^c : 25°S–25°N, Indian Ocean sector)

^a SSTA: changes in SST from the preindustrial to 2000 in ensemble of five CMIP5 models.

preindustrial level, but with aerosols specified from year 2000 of the "historical AA" run R_{aero} . Differences between these two experiments denote the aerosol-induced direct atmospheric responses from the preindustrial to 2000 $(R_{\rm dir} = R_{\rm aero} - R_{\rm clim})$. The atmospheric runs are 30–50 years long in different models. Results from the last 25 years for each model are used for analysis. By excluding the direct atmospheric responses in the coupled historical-AA simulations, we obtain the atmospheric circulation responses mediated by the aerosol-induced SST changes ($R_{\text{sst}} = R_{\text{total}}$ – R_{aero}). In terms of the decomposition method, previous studies showed it worked well in the North Pacific and North Atlantic (Shaw and Voigt 2015) and can be used in the analysis of Asian summer monsoon response to aerosol forcing (Li et al. 2018). However, Song et al. (2018a,b) noted that the decomposition may only work well in the zonal-mean sense in the atmospheric response to global warming, and Biasutti (2013) concluded that the decomposition did not work well in the Sahel region. Although the nonlinearity of the decomposition is not negligible, it does not influence the discussions in this analysis. Only the first-member run (r1i1p*) of each model is used to ensure equal weight in multimodel analysis. All model outputs are interpolated onto a common grid of 128 $(zonal) \times 64$ (meridional) grid points (about 2.8125° in the horizontal) and 22 vertical layers for easy comparison.

Furthermore, the SST-mediated atmospheric response to anthropogenic aerosol forcing is decomposed into a uniform cooling effect, interhemispheric asymmetry effect, and SST-patterned cooling effect over the tropical Indian Ocean via idealized AGCM experiments (Table 2) using the NOAA/GFDL Atmospheric Model, version 2.1 (AM2.1; Anderson et al. 2004). We use 2.5° longitude × 2° latitude horizontal resolution, with 24 vertical levels. Its convective parameterization is based on the relaxed Arakawa–Schubert scheme (Moorthi and Suarez 1992), and the cloud microphysics are parameterized by a single-moment

^b Tropical (25°S–25°N) annual-mean SST change from the preindustrial to 2000 in ensemble of five CMIP5 models.

^c Tropical (25°S–25°N) mean has been removed from the tropical Indian Ocean SST anomaly.

scheme based on Rotstayn (1997) and Rotstayn et al. (2000). In the AGCM experiments, the radiative forcing is fixed at the preindustrial level. The control simulation is run with the preindustrial climatological SST and sea ice concentration from the five CMIP5 models' ensemble. The forced experiments use the same radiative forcing and sea ice concentration as the control run, with different SST anomalies derived from the CMIP5 historical anthropogenic aerosol single-forcing simulations. The SST anomalies are the trends in the five CMIP5 models' ensemble from the preindustrial to 2000. All the experiments are run for 30 years after an initial spinup for a year. The differences between the forced experiments and the control run represent the SST feedback for the aerosol-induced Asian summer monsoon response.

Climate change from the preindustrial to 2000 is expressed using Sen's trend (Sen 1968) to eliminate the effect of extreme points. The Student's t test is used to estimate the statistical significance of the precipitation change to check the signal-to-noise confidence. To diagnose the characters of atmospheric circulation, we calculate the zonal-mean meridional streamfunction and the horizontal velocity potential using the wind components. The meridional streamfunction is defined in Eq. (1),

$$\psi_p(\theta, p) = \frac{2\pi \cos\theta}{g} \int_p^{ps} v dp, \qquad (1)$$

which integrates the meridional wind from the surface to a pressure level p.

Here ψ denotes the meridional streamfunction, θ represents the latitude, v is the meridional wind, and g is gravity constant. The velocity potential ϕ indicates the divergence (negative) and convergence (positive) of irrotational flow u_{ϕ} and v_{ϕ} defined as,

$$\begin{cases} u_{\phi} = \frac{\partial \phi}{\partial x} \\ v_{\phi} = \frac{\partial \phi}{\partial y} \end{cases}$$
 (2)

The net outgoing radiative flux at top of the atmosphere F_t is evaluated to investigate the radiative forcing effect of anthropogenic aerosols; U_{tl} , U_{ts} , D_{ts} indicate the upward longwave radiation, upward shortwave radiation, and downward shortwave radiation at the top of the atmosphere, respectively,

$$\Delta F_t = \Delta (U_{tl} + U_{ts} - D_{ts}). \tag{3}$$

3. Direct atmospheric response

Because of the localized emission sources and short residence time, anthropogenic aerosols are strongly

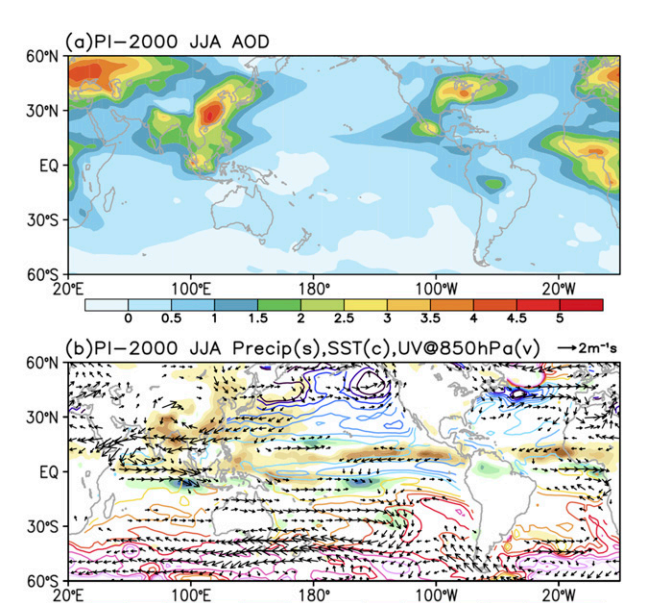


FIG. 1. (a) Global-mean AOD (ambient aerosol optical thickness at 550 nm; 1×10^{-1}) change from the preindustrial to 2000 in JJA. Data are from GFDL CM3. (b) Total response to aerosol changes from the preindustrial to 2000 in JJA: precipitation (shading; mm day⁻¹), SST [contours; 0.1°C interval with 0°C omitted; warm colors denote positive values; tropical mean (25°N–25°S) has been removed], and wind at 850 hPa (vectors; scale at top right; omitted where the magnitude $< 0.2 \, \text{m s}^{-1}$). Based on multimodel mean of CMIP5 historical-AA coupled simulations.

distributed geographically (Fig. 1a). Anthropogenic aerosol changes are mostly concentrated over Asia and Europe and to a lesser extent over Africa and the Americas since the Industrial Revolution.

Pronounced atmospheric circulation changes in response to anthropogenic aerosol forcing have been identified from coupled climate models and observations during the twentieth century, including anomalous cross-equatorial Hadley circulation and the corresponding southward shift of ITCZ (Allen et al. 2015; Wang et al. 2016a,b). Furthermore, Xu and Xie (2015) showed that the atmospheric temperature and circulation respond to aerosol forcing differently between boreal summer and winter. Figure 1b shows the multimodel ensemble mean of the SST, precipitation, and 850-hPa wind changes in response to anthropogenic aerosol forcing during boreal summer [June-August (JJA)] from the preindustrial to 2000 in CMIP5 historical-AA coupled simulations. Consistent with previous annual-mean results, aerosol-induced SST change shows a northsouth interhemispheric gradient with a maximum cooling centered over the North Pacific (Wang et al. 2016a). As required by the cross-equatorial energy transport (Kang et al. 2008; Chiang and Friedman

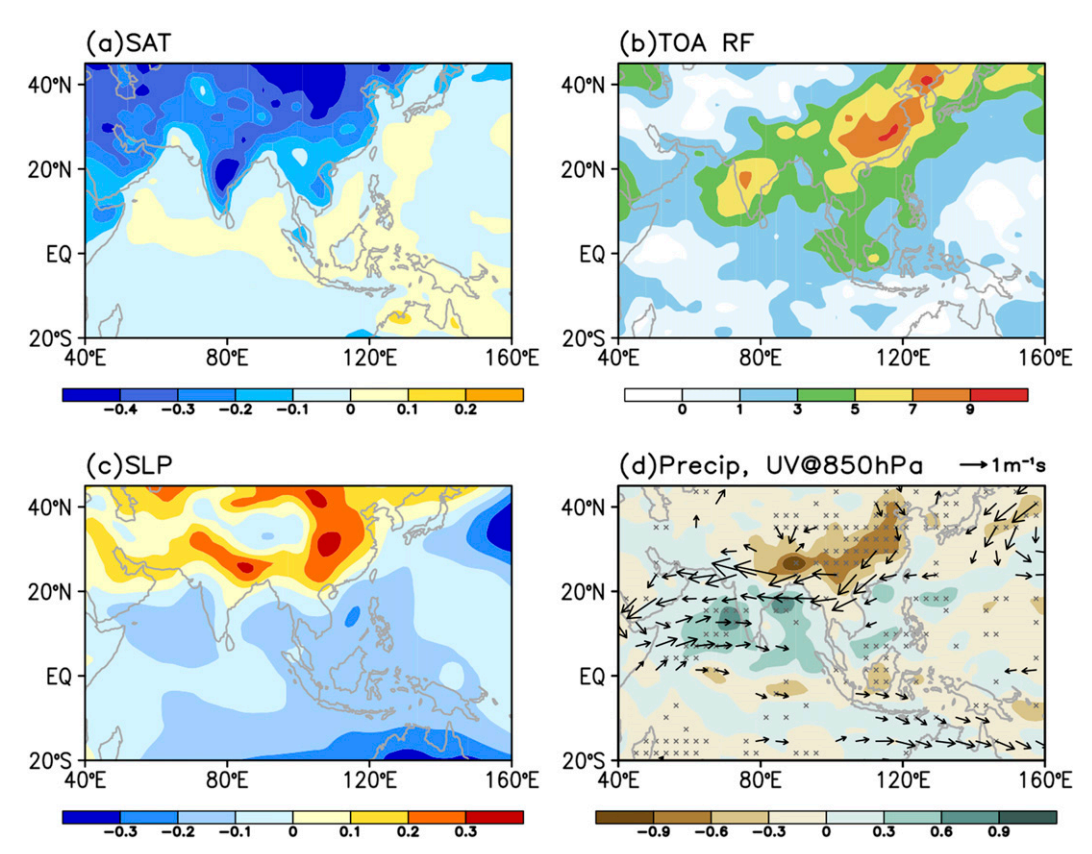


FIG. 2. Direct atmospheric response to aerosol changes from the preindustrial to 2000 in JJA: (a) SAT (°C), (b) TOA effective radiative forcing (W m⁻²), (c) SLP (hPa), (d) precipitation (mm day⁻¹) and wind at 850 hPa (vectors; scale at top right; omitted where the magnitude $< 0.2 \,\mathrm{m\,s^{-1}}$). Based on multimodel mean of $R_{\rm dir}$ with SST fixed at the preindustrial climatology. Hatched regions indicate precipitation changes exceed 90% statistical confidence.

2012; Kang et al. 2014), tropical rainfall decreases (increases) north (south) of the equator, representing a southward shift of the ITCZ (Hwang et al. 2013; Allen et al. 2015; Wang et al. 2016b).

Aside from the global interhemispheric asymmetry, anthropogenic aerosols weaken the Asian summer monsoon system (Fig. 1b), including the anomalous northeasterlies over East Asia and the northwestern Pacific, anomalous easterlies over South Asia, and anomalous westerlies over the equatorial Indian Ocean. The western Pacific subtropical high (WPSH) is closely related to the EASM change and may influence the SASM through atmospheric teleconnections (Lau et al. 2000; Zhou et al. 2009; Chen et al. 2016). Previous studies have linked the westward-extended WPSH with the corresponding EASM rainfall increase to both local and tropical Pacific SST warming (Lau et al. 2000; Zhou et al. 2009). Similarly, the aerosol-induced SST cooling over the Indo-western Pacific (IWP) causes the anomalous cyclonic circulation over the western North Pacific, which may lead to the weakening and eastward shift of WPSH (Fig. 1b). Besides, the aerosol forcing can also initiate the SST cooling over the midlatitude North Pacific, which causes a high pressure anomaly above the cool ocean (Fig. 1b). The anticyclonic circulation anomaly then induces stronger northeasterlies to the south and weakens the WPSH. A meridional wave pattern induced by this high pressure anomaly can further influence the circulation and rainfall over the tropical Indian Ocean (Chen et al. 2016). Consistent with the wind changes, precipitation decreases over East Asia, the northwestern Pacific, South Asia, and the north Indian Ocean, while increasing over the equatorial southeast Indian Ocean.

To investigate how the direct atmospheric response to radiative forcing regulates the aerosol-induced Asian summer monsoon responses, we first analyze the AGCM experiments. Conflicting views exist regarding the direct aerosol effect. With SST fixed at the preindustrial level, the concentration of anthropogenic aerosols over South Asia may lead to the surface cooling by the "solar dimming" effect (Ramanathan et al. 2005). Absorbing aerosols that lead to the atmospheric warming

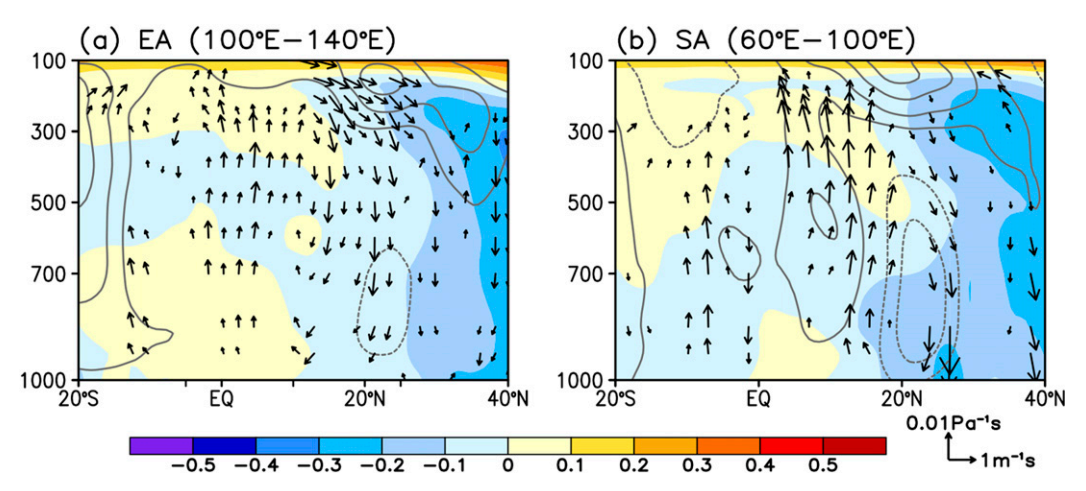


FIG. 3. Direct atmospheric response to aerosol changes from the preindustrial to 2000 in JJA: (a) East Asia ($100^{\circ}-140^{\circ}E$) and (b) South Asia ($60^{\circ}-100^{\circ}E$) zonal-mean air temperature (shading; °C), zonal wind (contours; $0.2 \,\mathrm{m\,s^{-1}}$ interval with $0 \,\mathrm{m\,s^{-1}}$ omitted; solid lines denote westerlies), meridional and vertical velocity (vectors; scale at bottom right; omitted where vertical motion response weaker than $1 \times 10^{-3} \,\mathrm{Pa\,s^{-1}}$). Based on multimodel mean of R_{dir} with SST fixed at the preindustrial climatology.

during boreal summer (Babu et al. 2002; Yang et al. 2009), on the other hand, can act as an "elevated heat pump" (EHP) to intensify Indian summer monsoon rainfall by enhancing the meridional temperature gradient (Lau and Kim 2006; Lau et al. 2006) and strengthening the EASM by both increasing the local land–sea surface thermal contrast and shifting the East Asian subtropical jet through fast adjustment without SST changes (Wang et al. 2017). The AGCM results show that the net (reflecting and absorbing) aerosol effect weakens most of the Asian summer monsoon except for the SASM over western India and the Bay of Bengal (Fig. 2).

In the direct atmospheric response, surface air temperature (SAT) decreases over the Eurasian continent (Fig. 2a), with little change over the ocean. Effective radiative forcing (ERF) at the top of the atmosphere resembles the aerosol optical depth (AOD) concentration very well over East and South Asia (Fig. 2b). By reflecting the shortwave radiation, aerosols cool the Asian land, thereby reducing the land-sea thermal contrast between the Asian continent and the adjacent oceans (Fig. 2a). The change in land-sea thermal contrast regulates the atmospheric circulation, characterized by a high surface pressure anomaly over the Asian continent and low sea level pressure (SLP) anomaly over the northwestern Pacific (Fig. 2c). Consistent with the SLP change, both EASM and SASM circulations weaken, with an anomalous northeasterly flow over southeast China and an anomalous easterly flow in South Asia around 20°N (Fig. 2d). Consistent with the atmospheric circulation response, Asia shows a general drying trend (Fig. 2d). However, the weakened Asian

summer monsoon circulation and associated rainfall decrease are limited on land north of 20°N (Li et al. 2018). Over the northwestern Pacific, the Indian Ocean, and south India, the direct response to aerosol forcing is weak. Over western India and the Bay of Bengal, precipitation increases in direct atmospheric response, inconsistent with the response pattern in coupled simulations (Fig. 1b). This is probably due to the effect of absorbing aerosols on atmospheric stability. Radiative heating of absorbing aerosols may cause warm air to rise. The upper-troposphere warm anomaly then act as an EHP, leading to the increased summer monsoon rainfall over South Asia by changing the atmospheric stability (Lau et al. 2006; Lau and Kim 2006).

The aerosol-induced land-sea thermal contrast drives the atmospheric overturning circulation. Figure 3 shows zonally averaged temperature and vertical motion changes in the East (100°-140°E) and South Asian (60°-100°E) sectors. Over East Asia, anthropogenic aerosols cool the whole troposphere north of 20°N. In thermal wind balance, the deep cooling structure over midlatitude East Asia anchors a westerly acceleration to the south in the upper troposphere (centered around 30°N at 200 hPa). An anomalous meridional overturning circulation develops with strong sinking motion between 20° and 40°N and rising motion between the equator and 20°N (Fig. 3a). Over the South Asian monsoon region, anthropogenic aerosols induce surface cooling (Fig. 2a), and the anomalous sinking motion develops north of 20°N (Fig. 3b). To the south over south India and the north tropical Indian Ocean, a strong increase in vertical motion in the mid- to upper troposphere in 5°-20°N

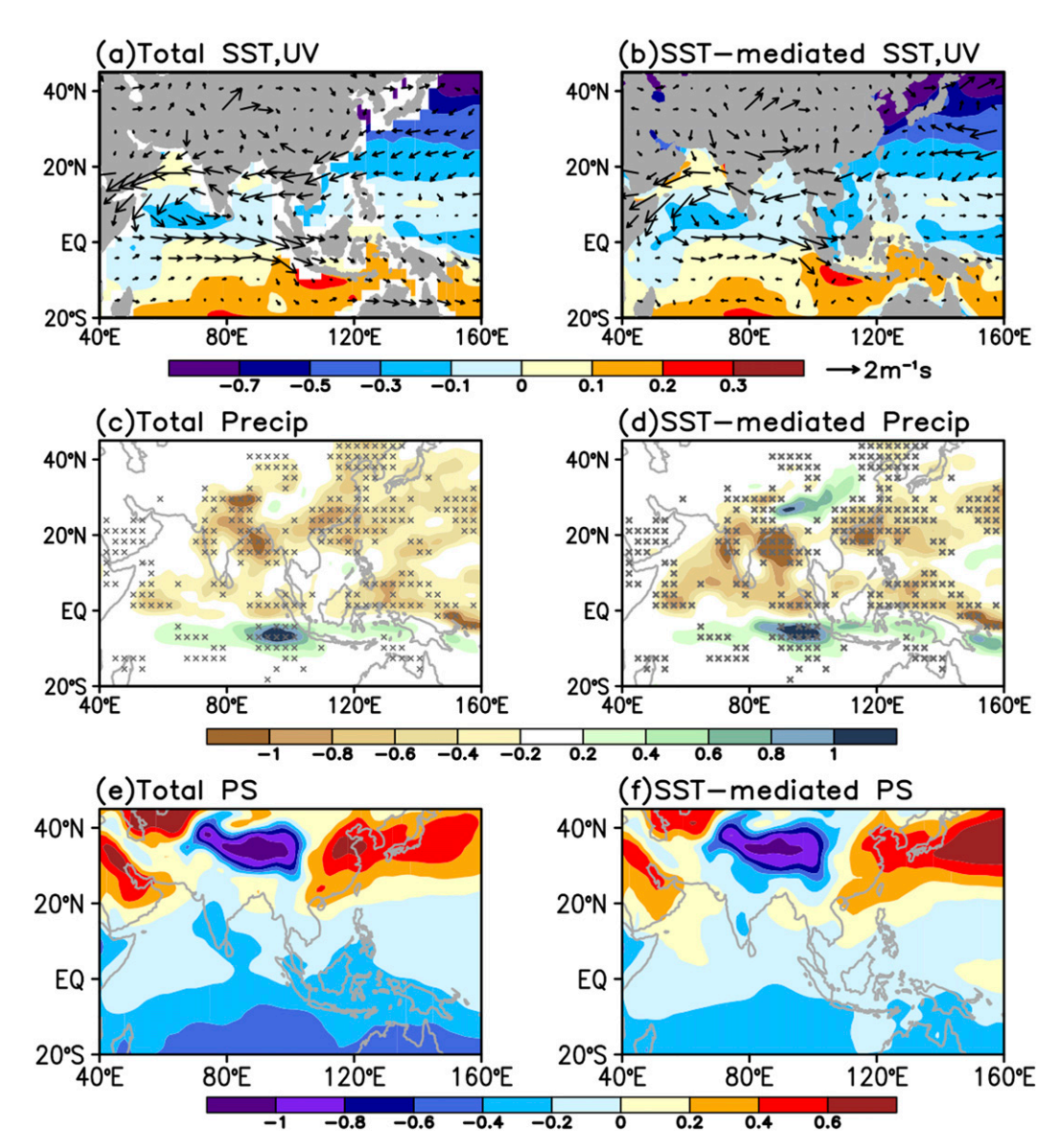


FIG. 4. (a),(c),(e) Total and (b),(d),(f) SST-mediated responses to aerosol changes from the preindustrial to 2000 in JJA: (a),(b) SST [shading; °C; tropical mean (25°N–25°S) has been removed] and wind at 850 hPa (vectors; scale at top right); (c),(d) precipitation (shading; mm day⁻¹); and (e),(f) SLP (shading; hPa). Based on multimodel means of R_{total} and R_{sst} . Hatched regions indicate precipitation changes exceed 90% statistical confidence.

(Fig. 3b) can be linked to the EHP effect (Lau et al. 2006; Lau and Kim 2006). On the south slope of the Tibetan Plateau, the air heated by absorbing aerosols leads to the strong upward motion in the upper troposphere and draws the warm and moist low-level inflow from the north Indian Ocean, resulting in the intensified rainfall over western India and the Bay of Bengal.

4. SST-mediated response

SST feedback is important in regulating the Asian summer monsoon response to aerosols. By differencing

the aerosol-induced total response and the direct atmospheric response, we isolate the SST feedback.

a. SST effect

The North Pacific is notably sensitive to anthropogenic aerosol forcing (Ming et al. 2011; Wang et al. 2013; Xie et al. 2013), with an intensified SST cooling east of Japan (Fig. 4b), downwind of major pollution sources (Chen et al. 2016). A large-scale high pressure anomaly in the lower troposphere (Fig. 4d) develops over the northwestern Pacific. The easterly anomalies

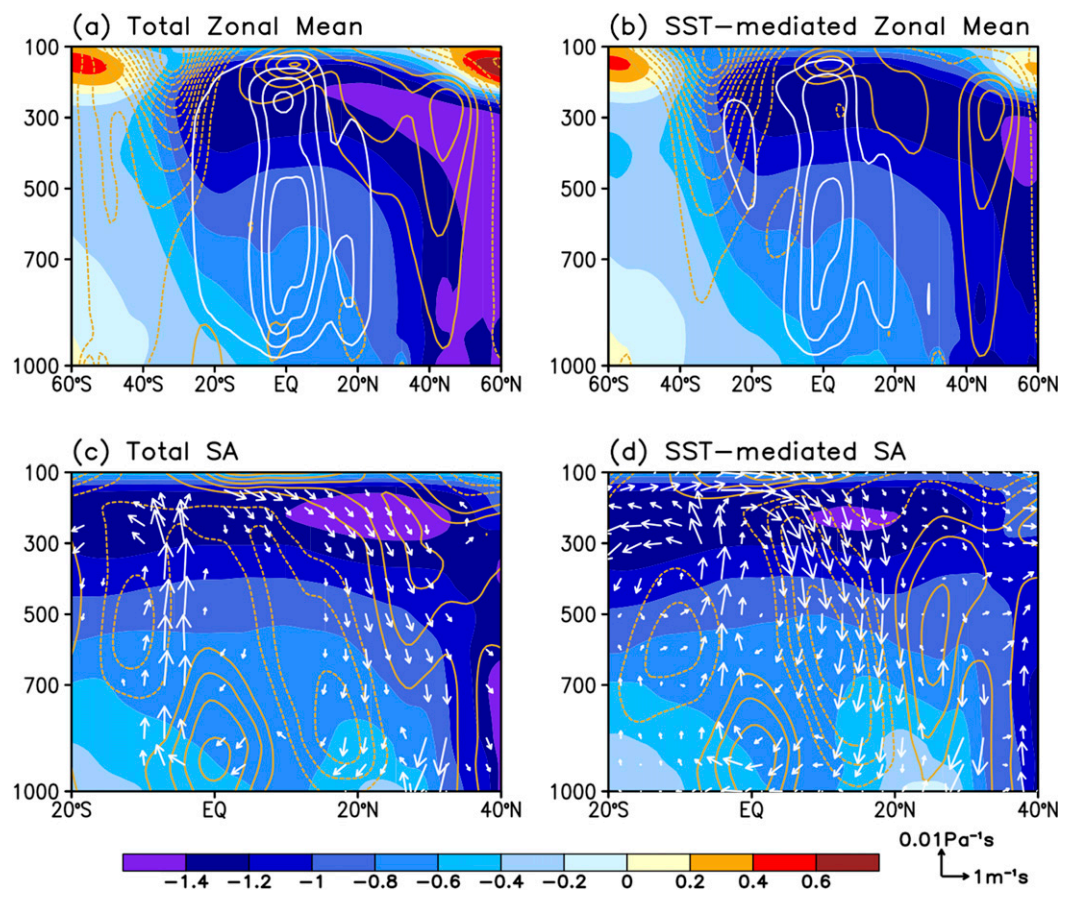


FIG. 5. (a),(c) Total and (b),(d) SST-mediated response to aerosol changes from the preindustrial to 2000 in JJA: (a),(b) Entire zonal-mean and (c),(d) South Asian (60° - 100° E) zonal-mean air temperature (shading; °C), zonal wind (yellow contours; $0.2 \,\mathrm{m\,s^{-1}}$ interval with $0 \,\mathrm{m\,s^{-1}}$ omitted; solid lines denote westerlies), meridional streamfunction [white contours in (a) and (b); $3 \times 10^{9} \,\mathrm{kg\,s^{-1}}$ interval with $0 \,\mathrm{kg\,s^{-1}}$ omitted; positive indicate clockwise circulation], and meridional and vertical velocity [vectors in (c) and (d); scale at bottom right; omitted where vertical velocity response weaker than $1 \times 10^{-3} \,\mathrm{Pa\,s^{-1}}$]. Based on multimodel means of R_{total} and R_{sst} .

on the south flank (near 20°N) weaken the climatological EASM monsoon circulation, and rainfall decreases over southeast China and the adjacent oceans (Fig. 4b). While the aerosol-induced total responses somewhat resemble the SST-mediated change over the ocean (Figs. 4a,b), precipitation change over inland East Asia (around 30°N) is positive in SST-mediated response, inconsistent with the total response (Fig. 4a). This is associated with the wind convergence between the low pressure anomaly on land and the high pressure anomaly over the northwestern Pacific induced by the SST cooling pattern (Figs. 4c,d). Aerosol-induced EASM circulation and precipitation changes north of 20°N are dominated by the direct atmospheric adjustments.

Over tropical South Asia and the Indian Ocean, aerosol-induced SASM changes are dominated by SST feedback (Figs. 4a,b). By removing the tropical-mean

cooling, the SST change shows both zonal and meridional asymmetry with relative cooling in the northwest and relative warming in the southeast tropical Indian Ocean. The zonal SST asymmetry is suggestive of Bjerknes feedback, which induces westerly anomalies on the equator, deepening the thermocline and reducing the SST cooling over the southeast tropical Indian Ocean (Xie et al. 2013). Corresponding to the SST pattern, an anomalous cyclonic circulation over the north Indian Ocean and south India weakens the climatological SASM. Rainfall decreases on and north of the equator while increasing over the southeast tropical Indian Ocean, consistent with the circulation change (Fig. 4).

To further validate how the aerosol-induced SST changes regulate the SASM responses, Fig. 5 shows the global and South Asia (60°–100°E) zonal-mean air temperature and meridional circulation changes in

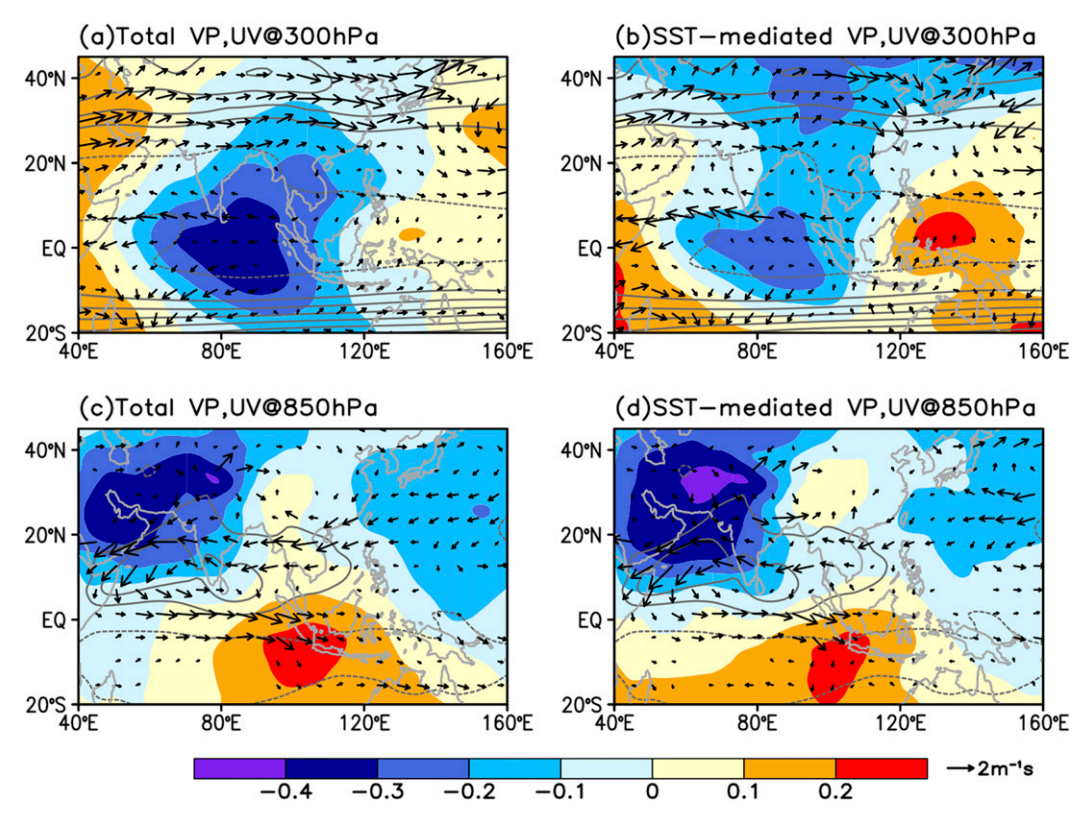


FIG. 6. (a),(c) Total and (b),(d) SST-mediated response to aerosol changes from the preindustrial to 2000 in JJA: (a),(b) 300 and (c),(d) 850-hPa velocity potential (shading; $10^6 \,\mathrm{m^2 \, s^{-1}}$) and wind (vectors; ; scale at bottom right; omitted where the magnitude < 0.1 m s⁻¹). Contours denote climatological-mean zonal winds (5 m s⁻¹ interval with 0 m s⁻¹ omitted; solid lines denote westerlies). Based on multimodel means of R_{total} and R_{sst} .

coupled and SST-mediated response. From an energy perspective, the spatial inhomogeneous anthropogenic aerosol forcing is much more efficient in causing circulation changes to compensate for the interhemispheric energy imbalance (Wang et al. 2016b). Anthropogenic aerosols induce a deep cooling structure over the Northern Hemisphere midlatitudes, mediated by the SST feedback (Figs. 5a,b; Xu and Xie 2015). According to the cross-equatorial energy transport theory (Kang et al. 2008; Chiang and Friedman 2012; Kang et al. 2014), the boreal-summer tropical meridional overturning circulation, of which the SASM is a major part (Chen et al. 2006; Bollasina et al. 2011), weakens to reduce the energy flow to the Southern Hemisphere and thus alleviates the interhemispheric asymmetry (Figs. 5c,d). The anomalous sinking motion generated by the SST feedback reduces the ascent over the north Indian Ocean and South Asia, opposing the local Hadley circulation, and leads to the rainfall decrease over the tropical SASM region. The anomalous rising motion is centered over 10°S-0°, contributing to the rainfall increase over the tropical southeast Indian Ocean.

Besides the regional meridional atmospheric overturning circulation change, the aerosol-induced SST feedback also anchors an anomalous westerly acceleration in the midlatitude Northern Hemisphere in thermal wind balance (Figs. 5a,b). To diagnose the atmospheric circulation change in horizontal view, we calculate the velocity potential and the wind change in the upper (300 hPa) and lower (850 hPa) troposphere. In tropical South Asia, there is a strong local divergent flow in the upper troposphere (Figs. 6a,b), and the corresponding northwest-southeast divergence-convergence dipole center in the lower troposphere (Figs. 6c,d), featuring the weakening of the local meridional atmospheric overturning circulation. Furthermore, the aerosol-induced SST cooling pattern also excites an anomalous zonal circulation, with stronger ascent over the tropical southeastern Indian Ocean and weaker descent to the east (Bollasina et al. 2011), leading to the rainfall decrease over the Indo-Pacific Maritime Continent regions (Figs. 4, 6). In the extratropics, the climatological westerlies are accelerated and shift a little bit southward because of the SST feedback (Fig. 6). Although the SSTmediated westerly adjustment effect is weak on South

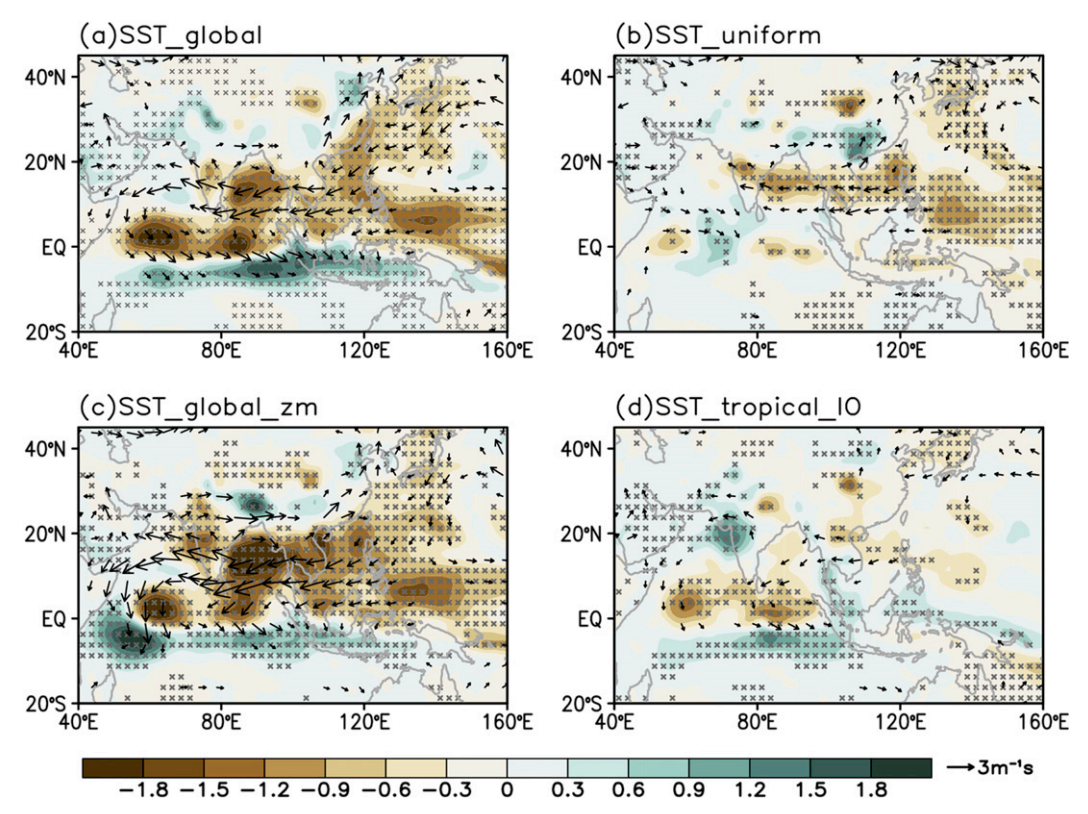


FIG. 7. Aerosol-induced SST-mediated changes in precipitation (shading; mm day $^{-1}$) and 850-hPa wind (vectors; wind speed $< 0.3 \,\mathrm{m\,s^{-1}}$ omitted) in JJA in AM2.1 experiments forced with different SST patterns: (a) global SST changes, (b) SST uniform cooling, (c) global zonal-mean SST changes, and (d) tropical Indian Ocean SST changes with tropical-mean SST change removed. Hatched regions indicate precipitation changes exceed 90% statistical confidence.

Asia rainfall, it is important for the rainfall increase centered around 30°N, 90°E (Figs. 4b, 6b,d).

b. SST patterns

Using historical-AA coupled simulations and "fixed SST" AGCM runs, we have shown that the SST adjustment is important for the SASM response to anthropogenic aerosol forcing. Previous studies showed that the SST-pattern effect (warmer get wetter; Xie et al. 2010) and the global SST change (wet get wetter; Held and Soden 2006) are both important for the seasonal-mean rainfall change (Huang et al. 2013). In the wet-getwetter view, the spatially uniform SST warming causes rainfall to increase in the climatological rainy regions. We perform a suite of AGCM experiments to investigate the mechanisms by which the aerosol-induced SST feedback regulates the Asian summer monsoon.

Figure 7a shows the precipitation and 850-hPa wind change due to an aerosol-induced global SST anomaly in GFDL AM2.1. The results resemble those from the CMIP5 multimodel ensemble (Fig. 4b), though the decrease in precipitation over India and the Arabian Sea in

GFDL AM2.1 is much weaker. There is a possibility that this is due to the parameterization of GFDL AM2.1, but equally possible are different representations of circulation and air-sea interaction between GFDL AM2.1 and CMIP5 models. A number of additional experiments were performed (Table 2). First, we forced the AGCM with a uniform cooling of -0.51° C (based on the tropical-mean SST change in the CMIP5 ensemble mean of the historical-AA runs) superposed on the climatological SST. Figure 7b shows the precipitation and 850-hPa wind changes. The wet-get-wetter effect is obvious with significant rainfall decrease limited over 10°-20°N, 80°-120°E, where climatological convection is strong during boreal summer (Tan et al. 2008; Huang et al. 2013). Compared with the global SST pattern (Fig. 7a), the uniform SST cooling effect on SASM precipitation and wind is weak.

Previous studies indicated that both the local SST in the tropical Indian Ocean (Ganguly et al. 2012a; Xie et al. 2013) and the global meridional temperature gradient (Xu and Xie 2015; Wang et al. 2016a) contribute to the decreased SASM precipitation and circulation.

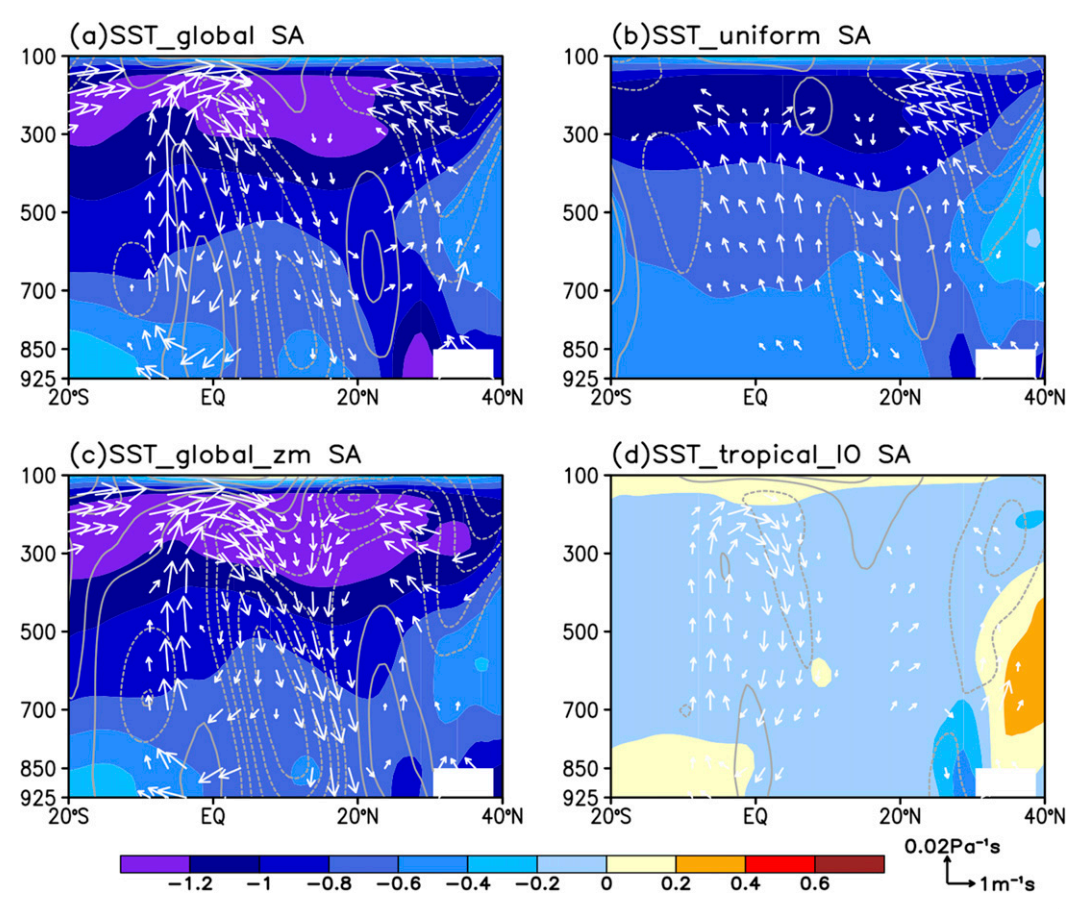


FIG. 8. Aerosol-induced SST-mediated changes in air temperature (shading; K), zonal wind (contours at $0.3~{\rm m\,s^{-1}}$ interval with $0~{\rm m\,s^{-1}}$ omitted), and meridional and vertical velocity (vectors; scale at bottom right; omitted where vertical velocity response is weaker than $2\times10^{-3}~{\rm Pa\,s^{-1}}$) averaged zonally over the South Asian sector (60° – 100° E) in JJA in AM2.1 experiments forced with different SST patterns: (a) global SST changes, (b) SST uniform cooling, (c) global zonal-mean SST changes, and (d) tropical Indian Ocean SST changes with tropical mean SST change removed.

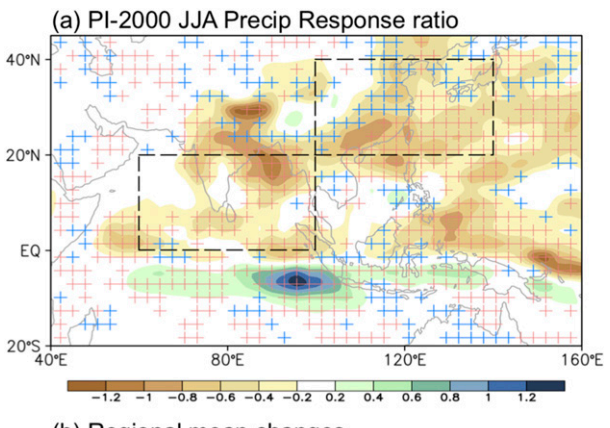
To examine the interhemispheric SST gradient effect, we forced the AGCM with the global zonal-mean SST anomaly (Fig. 7c). Similarity in precipitation and 850-hPa wind response patterns between Figs. 7a and 7c indicates that the interhemispheric SST gradient dominates the SST feedback for the SASM response. The regional SST cooling pattern effect is further examined with an AGCM forced by the tropical Indian Ocean SST anomaly with its tropical-mean trend removed (Fig. 7d). The precipitation and wind response patterns in the tropical Indian Ocean in Fig. 7d are similar to that in Figs. 7a and 7c, verifying the regional oceanatmosphere coupled response regulated by Bjerknes feedback. Compared with the north-south interhemispheric SST gradient, the Bjerknes effect over the tropical Indian Ocean on SASM is weak.

By averaging the zonal-mean air temperature and circulation changes over South Asia (60°-100°E), we

further investigate the atmospheric circulation responses to different SST forcing patterns. Though the temperature responses show some disparities in Figs. 8a and 5d, the atmospheric circulation change forced by the global SST response pattern resembles that in CMIP5 multimodel ensemble-mean results. The SST uniform cooling effect, however, has only a weak effect on the large-scale monsoon circulation (Fig. 8b). Comparison of Figs. 8a, 8c, and 8d highlights the important role of aerosol-induced north—south interhemispheric temperature gradient in altering the local atmospheric overturning circulation.

5. Relative contribution

Our decomposition analysis separated the distinct Asian summer monsoon response processes to anthropogenic aerosol forcing, revealing how the direct atmospheric response and the SST feedback shape



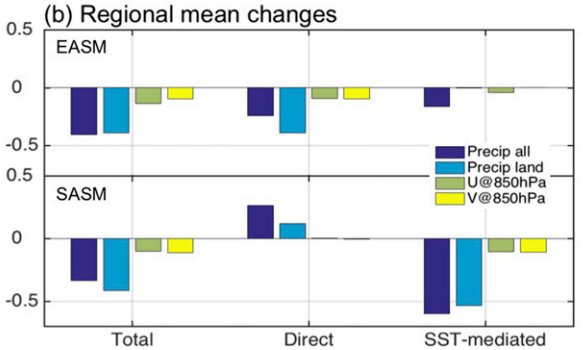


FIG. 9. (a) Total precipitation (shading; mm day⁻¹) response to aerosol changes from the preindustrial to 2000 in JJA and the precipitation response ratio (red and blue crosses respectively denote the SST-mediated response direct atmospheric response dominates over the other one; absolute values < 0.3 omitted). (b) Regional-mean changes [boxes in (a)] of precipitation (mm day⁻¹) and zonal and meridional winds at 850 hPa (m s⁻¹) in total, direct, and SST-mediated responses in EASM (20°–40°N, 100°–140°E) and SASM (0°–20°N, 60°–100°E).

the weakening of Asian summer monsoon in different regions.

To evaluate the relative contribution of direct atmospheric response and SST feedback to the Asian summer monsoon response to anthropogenic aerosol forcing, we further calculate the precipitation response ratio (Samset et al. 2016),

$$R_{\text{precip}} = \frac{|\Delta P_{\text{SST}}| - |\Delta P_{\text{dir}}|}{|\Delta P_{\text{SST}}| + |\Delta P_{\text{dir}}|}.$$
 (4)

Here $\Delta P_{\rm SST}$ and $\Delta P_{\rm dir}$ denote the SST-mediated and direct Asian summer monsoon precipitation response to anthropogenic aerosol forcing. Positive values in Fig. 9a indicate that the SST feedback dominates over the direct atmospheric response in aerosol-induced precipitation change (absolute precipitation ratio < 0.3; omitted) and vice versa. Over East Asia and the adjacent oceans, rainfall decreases the most over southeast China land regions and to a lesser extent over the northwestern

Pacific. The precipitation response ratio highlights the dominance of direct atmospheric response in rainfall change over East Asia land regions (blue crosses in Fig. 9a). However, decreased rainfall over the northwestern Pacific is mediated by the aerosol-induced SST cooling pattern (Fig. 4b). In South Asia and the tropical Indian Ocean, the rainfall decrease south of 20°N is mediated by the aerosol-induced SST change alone (red crosses in Fig. 9a).

We further examine the regional-mean rainfall and wind changes at 850-hPa level. Over the EASM region (20°-40°N, 100°-140°E), the direct atmospheric response to radiative forcing contributes about 59% of the total rainfall decrease, while the contribution from the SST feedback is about 39%. Over inland East Asia, the rainfall decrease is dominated by the direct atmospheric response (Fig. 9b). For the EASM monsoon circulation change, zonal wind anomalies are mediated by the direct atmospheric response (69%) compared with the rainfall change. However, the SST feedback contributes only about 31% of the EASM zonal wind response, with little effect on the anomalous meridional winds (Figs. 4b, 9b). Over the tropical SASM region (0°–20°N, 60°E-100°E), total and land precipitation changes to anthropogenic aerosol forcing contradict each other in the direct atmospheric response and the SST-mediated response (Fig. 9b). Considering the zonal and meridional wind changes, the aerosol-induced SST feedback in the tropical Indian Ocean opposes the direct atmospheric adjustment effect, leading to the weakened SASM.

6. Summary and discussion

Unlike GHGs that induce strong atmospheric moistening through SST increase, anthropogenic aerosols affect the monsoon precipitation largely through changes in atmospheric circulation (Li et al. 2015). In this study, we have investigated how anthropogenic aerosol forcing regulates the atmospheric circulation change of Asian summer monsoon via different physical processes and evaluated their relative contributions. Specifically, we show that the aerosol-induced interhemispheric SST gradient dominates the monsoonal precipitation response.

Using multiple coupled climate models forced by the anthropogenic aerosols and idealized AGCM experiments, we confirmed the robust drying trend and weakened Asian summer monsoon circulation since the industrial revolution and identified the distinct response mechanisms of EASM and SASM. Our decomposition of aerosol-induced climate change shows that the weakened EASM rainfall and circulation are dominated by the direct atmospheric response, while the weakened SASM

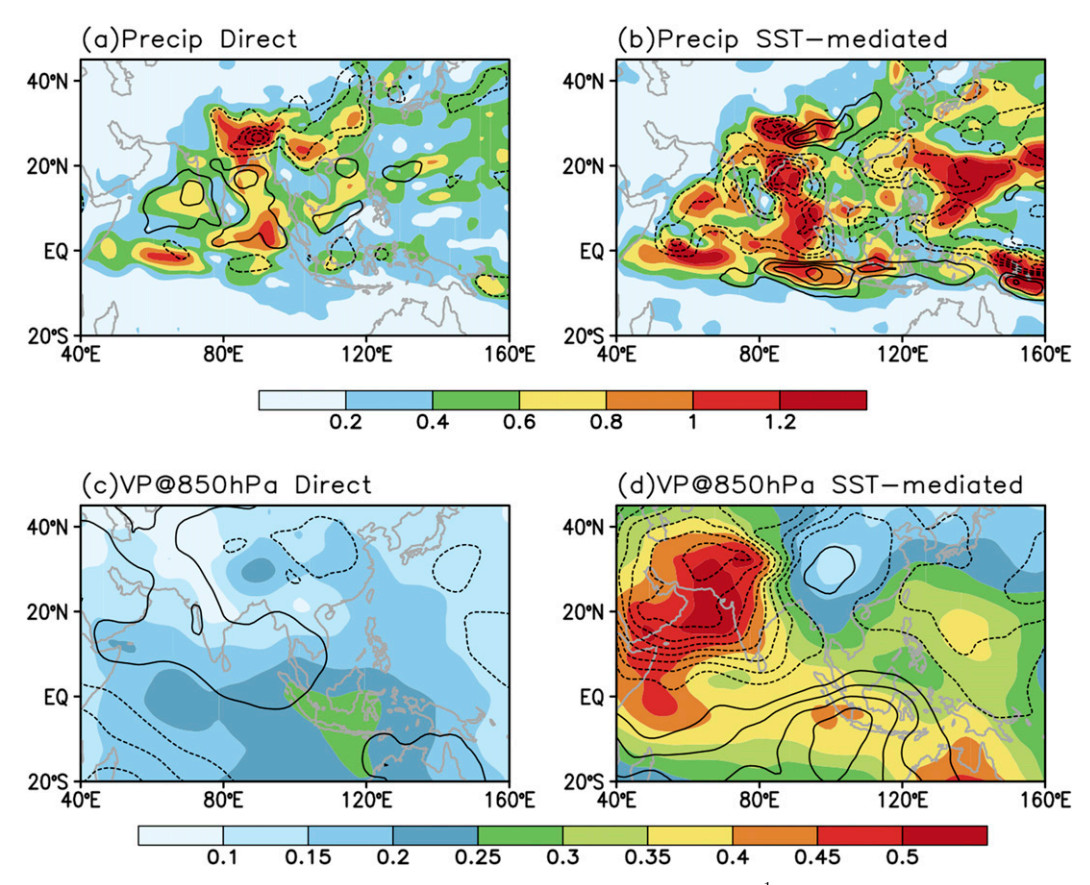


FIG. 10. CMIP5 intermodel spread (shading) of (a),(b) precipitation (mm day $^{-1}$) and (c),(d) velocity potential at 850 hPa ($\times 10^6$ m 2 s $^{-1}$) in (a),(c) direct atmospheric and (b),(d) SST-mediated responses, along with the ensemblemean change [contours; 0.3 mm day $^{-1}$ interval in (a) and (b) and 0.05×10^6 m 2 s $^{-1}$ interval in (c) and (d), with 0 m 2 s $^{-1}$ omitted] in JJA.

is regulated mostly by the SST feedback. In the direct atmospheric response, anthropogenic aerosols induce the cooling of local land surface, reducing land—sea thermal contrast. The reduced land—sea thermal contrast generates the anomalous high pressure over the Asian land region north of 20°N, with the anomalous sinking motion between 20° and 40°N.

Anthropogenic aerosol forcing causes the SST decrease globally, with considerable spatial patterns. AGCM experiments show the importance of the aerosol-induced SST cooling pattern in the Asian summer monsoon change. Regional cooling of SST over the North Pacific also contributes to the weakened EASM over the tropical northwestern Pacific, but its effect is weak over inland East Asia. Over the tropical Indian Ocean and South Asia, the SASM response to anthropogenic aerosol forcing is dominated by the SST feedback. The north—south interhemispheric asymmetry in aerosol-induced SST response plays a dominant role in causing the tropical atmospheric overturning circulation to weaken over the SASM region. The SST-mediated response features

an anomalous sinking (rising) motion north (south) of the equator, dominating the weakened SASM circulation and the precipitation decrease. A regional SST cooling pattern in the tropical Indian Ocean also contributes to the weakened SASM through Bjerknes feedback, although the amplitude is much weaker.

Aerosols are the largest source of uncertainty in radiative forcing during the instrumental era because of insufficient understanding of indirect microphysical effects on cloud and precipitation (Boucher et al. 2013). Compared to the MODIS observations, the AOD seems to be underestimated over South Asia, while overestimated over East Asia (Remer et al. 2008). This may create biases in the top-of-the-atmosphere (TOA) ERF and further influence our conclusions regarding the distinct impact of direct atmospheric response versus SST-mediated response in EASM and SASM changes. How the discrepancy between climate models and observations may affect the Asian summer monsoon response deserves further study with improved models and more targeted experiments. Besides, the intermodel

uncertainty is indeed large in the direct atmospheric response over the Asian summer monsoon regions, but the uncertainty due to the SST feedback is as large over the SASM region (Fig. 10). In fact, the latter is overall larger than the former over the broad Indo—western Pacific region, for example, the Maritime Continent. This also points to the need to study large-scale coupled response to aerosols and radiative forcing in general, including the effect on the atmospheric circulation (Xie et al. 2015; Collins et al. 2018).

Acknowledgments. This work is supported by the National Natural Science Foundation of China (Grants 41806006, 41876006); China Postdoctoral Science Foundation (Grant 2018M632720); the State Key Laboratory of Tropical Oceanography, South China Sea Institute of Oceanology, Chinese Academy of Sciences (Grant LTO1804); and the NSFC-Shandong Joint Fund for Marine Science Research Centers (U1406401). Shang-Ping Xie is supported by the U.S. National Science Foundation and Yu Kosaka is supported by the Japan Society for the Promotion of Science (Grant 18H01278), Belmont Forum CRA "InterDec," and Integrated Research Program for Advancing Climate Models. We acknowledge the WCRP Working Group on Coupled Modeling, which is responsible for CMIP, and the climate modeling groups (listed in Table 1 of this paper) for producing and making available the model outputs. The National Oceanic and Atmospheric Administration (NOAA)/Geophysical Fluid Dynamics Laboratory (GFDL) provided computer codes and related datasets of the AM2.1 model.

REFERENCES

- Allen, R. J., A. T. Evan, and B. B. Booth, 2015: Interhemispheric aerosol radiative forcing and tropical precipitation shifts during the late twentieth century. J. Climate, 28, 8219–8246, https://doi.org/10.1175/JCLI-D-15-0148.1.
- Anderson, J. L., and Coauthors, 2004: The new GFDL global atmosphere and land model AM2-LM2: Evaluation with prescribed SST simulations. *J. Climate*, **17**, 4641–4673, https://doi.org/10.1175/JCLI-3223.1.
- Babu, S. S., S. K. Satheesh, and K. K. Moorthy, 2002: Aerosol radiative forcing due to enhanced black carbon at an urban site in India. *Geophys. Res. Lett.*, 29, 1880, https://doi.org/10.1029/2002GL015826.
- Bao, Z., Z. Wen, and R. Wu, 2009: Variability of aerosol optical depth over east Asia and its possible impacts. J. Geophys. Res., 114, D05203, https://doi.org/10.1029/2008JD010603.
- Biasutti, M., 2013: Forced Sahel rainfall trends in the CMIP5 archive. J. Geophys. Res. Atmos., 118, 1613–1623, https://doi.org/10.1002/jgrd.50206.
- Bollasina, M. A., Y. Ming, and V. Ramaswamy, 2011: Anthropogenic aerosols and the weakening of the South Asian summer

- monsoon. *Science*, **334**, 502–505, https://doi.org/10.1126/science.1204994.
- ——, and ——, 2013: Earlier onset of the Indian monsoon in the late twentieth century: The role of anthropogenic aerosols. *Geophys. Res. Lett.*, **40**, 3715–3720, https://doi.org/10.1002/grl.50719.
- —, —, M. D. Schwarzkopf, and V. Naik, 2014: Contribution of local and remote anthropogenic aerosols to the twentieth century weakening of the South Asian monsoon. *Geophys. Res. Lett.*, **41**, 680–687, https://doi.org/10.1002/2013GL058183.
- Booth, B. B., N. J. Dunstone, P. R. Halloran, T. Andrews, and N. Bellouin, 2012: Aerosols implicated as a prime driver of twentieth-century North Atlantic climate variability. *Nature*, 484, 228–232, https://doi.org/10.1038/nature10946; Corrigendum, 485, 534, https://doi.org/10.1038/nature11138.
- Boucher, O., and Coauthors, 2013: Clouds and aerosols. *Climate Change 2013: The Physical Science Basis*, T. F. Stocker et al., Eds., Cambridge University Press, 571–657, https://www.ipcc.ch/site/assets/uploads/2018/02/WG1AR5_Chapter07_FINAL-1.pdf.
- Chang, C.-Y., J. C. H. Chiang, M. F. Wehner, A. R. Friedman, and R. Ruedy, 2011: Sulfate aerosol control of tropical Atlantic climate over the twentieth century. *J. Climate*, 24, 2540–2555, https://doi.org/10.1175/2010JCLI4065.1.
- Chen, J.-P., I.-J. Chen, and I.-C. Tsai, 2016: Dynamic feedback of aerosol effects on the East Asian summer monsoon. *J. Climate*, 29, 6137–6149, https://doi.org/10.1175/JCLI-D-15-0758.1.
- Chen, T.-C., 2006: Variation of the Asian monsoon water vapor budget: Interaction with the global-scale modes. *The Asian Monsoon*, B. Wang, Ed., Springer/Praxis Publishing, 417–457, https://doi.org/10.1007/3-540-37722-0.
- Chiang, J. C. H., and A. R. Friedman, 2012: Extratropical cooling, interhemispheric thermal gradients, and tropical climate change. *Annu. Rev. Earth Planet. Sci.*, 40, 383–412, https://doi.org/10.1146/annurev-earth-042711-105545.
- Collins, M., and Coauthors, 2013: Long-term climate change: Projections, commitments and irreversibility. *Climate Change 2013: The Physical Science Basis*, T. F. Stocker et al., Eds., Cambridge University Press, 1029–1136, https://www.ipcc.ch/site/assets/uploads/2018/02/WG1AR5_Chapter12_FINAL.pdf.
- —, and Coauthors, 2018: Challenges and opportunities for improved understanding of regional climate dynamics. *Nat. Climate Change*, 8, 101–108, https://doi.org/10.1038/s41558-017-0059-8.
- Dong, B., and R. Sutton, 2015: Dominant role of greenhouse-gas forcing in the recovery of Sahel rainfall. *Nat. Climate Change*, 5, 757–760, https://doi.org/10.1038/nclimate2664.
- ——, R. T. Sutton, E. J. Highwood, and L. J. Wilcox, 2016: Preferred response of the East Asian summer monsoon to local and non-local anthropogenic sulphur dioxide emissions. *Climate Dyn.*, 46, 1733–1751, https://doi.org/10.1007/s00382-015-2671-5.
- Donner, L. J., and Coauthors, 2011: The dynamical core, physical parameterizations, and basic simulation characteristics of the atmospheric component of the GFDL global coupled model CM3. J. Climate, 24, 3484–3519, https://doi.org/10.1175/2011JCL13955.1.
- Ganguly, D., P. J. Rasch, H. Wang, and J.-H. Yoon, 2012a: Climate response of the South Asian monsoon system to anthropogenic aerosols. J. Geophys. Res., 117, D13209, https://doi.org/ 10.1029/2012JD017508.
- ——, ——, and ——, 2012b: Fast and slow responses of the South Asian monsoon system to anthropogenic aerosols. *Geophys. Res. Lett.*, **39**, L18804, https://doi.org/10.1029/2012GL053043.

- Gong, D.-Y., and S.-W. Wang, 2000: Severe summer rainfall in China associated with enhanced global warming. *Climate Res.*, **16**, 51–59, https://doi.org/10.3354/cr016051.
- Hansen, J., and Coauthors, 2005: Efficacy of climate forcings. J. Geophys. Res., 110, D18104, https://doi.org/10.1029/ 2005JD005776.
- Held, I. M., and B. J. Soden, 2006: Robust responses of the hydrological cycle to global warming. *J. Climate*, 19, 5686–5699, https://doi.org/10.1175/JCLI3990.1; Corrigendum, 24, 1559–1560, https://doi.org/10.1175/2010JCLI4045.1.
- —, T. L. Delworth, J. Lu, K. L. Findell, and T. R. Knutson, 2005: Simulation of Sahel drought in the 20th and 21st centuries. *Proc. Natl. Acad. Sci. USA*, **102**, 17891–17896, https://doi.org/10.1073/pnas.0509057102.
- Huang, P., S.-P. Xie, K. Hu, G. Huang, and R. Huang, 2013: Patterns of the seasonal response of tropical rainfall to global warming. *Nat. Geosci.*, 6, 357–361, https://doi.org/10.1038/ngeo1792.
- Hwang, Y.-T., D. M. W. Frierson, and S. M. Kang, 2013: Anthropogenic sulfate aerosol and the southward shift of tropical precipitation in the late 20th century. *Geophys. Res. Lett.*, 40, 2845–2850, https://doi.org/10.1002/grl.50502.
- Kang, S. M., I. M. Held, D. M. W. Frierson, and M. Zhao, 2008: The response of the ITCZ to extratropical thermal forcing: Idealized slab-ocean experiments with a GCM. J. Climate, 21, 3521– 3532, https://doi.org/10.1175/2007JCLI2146.1.
- —, and S.-P. Xie, 2014: Contrasting the tropical responses to zonally asymmetric extratropical and tropical thermal forcing. *Climate Dyn.*, 42, 2033–2043, https://doi.org/10.1007/ s00382-013-1863-0.
- Kaufman, Y. J., D. Tanré, and O. Boucher, 2002: A satellite view of aerosols in the climate system. *Nature*, 419, 215–223, https:// doi.org/10.1038/nature01091.
- Lamarque, J.-F., and Coauthors, 2010: Historical (1850–2000) gridded anthropogenic and biomass burning emissions of reactive gases and aerosols: Methodology and application. Atmos. Chem. Phys., 10, 7017–7039, https://doi.org/10.5194/acp-10-7017-2010.
- Lau, K.-M., and K.-M. Kim, 2006: Observational relationships between aerosol and Asian monsoon rainfall, and circulation. *Geophys. Res. Lett.*, 33, L21810, https://doi.org/10.1029/ 2006GL027546.
- —, and —, 2017: Competing influences of greenhouse warming and aerosols on Asian summer monsoon circulation and rainfall. Asia-Pac. J. Atmos. Sci., 53, 181–194, https://doi.org/ 10.1007/s13143-017-0033-4.
- —, and S. Yang, 2000: Dynamical and boundary forcing characteristics of regional components of the Asian summer monsoon. *J. Climate*, 13, 2461–2482, https://doi.org/10.1175/ 1520-0442(2000)013<2461:DABFCO>2.0.CO;2.
- —, M. K. Kim, and K.-M. Kim, 2006: Asian summer monsoon anomalies induced by aerosol direct forcing: The role of the Tibetan Plateau. *Climate Dyn.*, 26, 855–864, https://doi.org/ 10.1007/s00382-006-0114-z.
- Li, X., M. Ting, C. Li, and N. Henderson, 2015: Mechanisms of Asian summer monsoon changes in response to anthropogenic forcing in CMIP5 models. *J. Climate*, 28, 4107–4125, https:// doi.org/10.1175/JCLI-D-14-00559.1.
- —, and D. E. Lee, 2018: Fast adjustments of the Asian summer monsoon to anthropogenic aerosols. *Geophys. Res. Lett.*, **45**, 1001–1010, https://doi.org/10.1002/2017GL076667.
- Li, Z., and Coauthors, 2016: Aerosol and monsoon climate interactions over Asia. Rev. Geophys., 54, 866–929, https:// doi.org/10.1002/2015RG000500.

- Ma, S., and Coauthors, 2017: Detectable anthropogenic shift toward heavy precipitation over eastern China. J. Climate, 30, 1381–1396, https://doi.org/10.1175/JCLI-D-16-0311.1.
- Menon, S., J. Hansen, L. Nazarenko, and Y. Luo, 2002: Climate effects of black carbon aerosols in China and India. *Science*, 297, 2250–2253, https://doi.org/10.1126/science.1075159.
- Ming, Y., and V. Ramaswamy, 2011: A model investigation of aerosol-induced changes in tropical circulation. *J. Climate*, 24, 5125–5133, https://doi.org/10.1175/2011JCLI4108.1.
- —, —, and G. Chen, 2011: A model investigation of aerosolinduced changes in boreal winter extratropical circulation. *J. Climate*, 24, 6077–6091, https://doi.org/10.1175/2011JCLI4111.1.
- Moorthi, S., and M. J. Suarez, 1992: Relaxed Arakawa–Schubert: A parameterization of moist convection for general circulation models. *Mon. Wea. Rev.*, 120, 978–1002, https://doi.org/10.1175/ 1520-0493(1992)120<0978:RASAPO>2.0.CO:2.
- Piao, S., and Coauthors, 2010: The impacts of climate change on water resources and agriculture in China. *Nature*, **467**, 43–51, https://doi.org/10.1038/nature09364.
- Qian, Y., M. G. Flanner, L. R. Leung, and W. Wang, 2011: Sensitivity studies on the impacts of Tibetan Plateau snowpack pollution on the Asian hydrological cycle and monsoon climate. *Atmos. Chem. Phys.*, 11, 1929–1948, https://doi.org/10.5194/acp-11-1929-2011.
- Ramanathan, V., and Coauthors, 2005: Atmospheric brown clouds: Impacts on South Asian climate and hydrological cycle. *Proc. Natl. Acad. Sci. USA*, **102**, 5326–5333, https://doi.org/10.1073/pnas.0500656102.
- Remer, L. A., and Coauthors, 2008: Global aerosol climatology from the MODIS satellite sensors. J. Geophys. Res., 113, D14S07, https://doi.org/10.1029/2007JD009661.
- Richardson, T. B., P. M. Forster, T. Andrews, and D. J. Parker, 2016: Understanding the rapid precipitation response to CO₂ and aerosol forcing on a regional scale. *J. Climate*, **29**, 583–594, https://doi.org/10.1175/JCLI-D-15-0174.1.
- Rosenfeld, D., U. Lohmann, G. B. Raga, C. D. O'Dowd, M. Kulmala, S. Fuzzi, A. Reissell, and M. O. Andreae, 2008: Flood or drought: How do aerosols affect precipitation? *Science*, 321, 1309–1313, https://doi.org/10.1126/science.1160606.
- Rotstayn, L. D., 1997: A physically based scheme for the treatment of stratiform clouds and precipitation in large-scale models. I: Description and evaluation of microphysical processes. *Quart. J. Roy. Meteor. Soc.*, **123**, 1227–1282, https://doi.org/10.1002/qj.49712354106.
- ——, B. F. Ryan, and J. J. Katzfey, 2000: A scheme for calculation of the liquid fraction in mixed-phase clouds in large-scale models. *Mon. Wea. Rev.*, **128**, 1070–1088, https://doi.org/10.1175/1520-0493(2000)128<1070:ASFCOT>2.0.CO;2.
- Samset, B. H., and Coauthors, 2016: Fast and slow precipitation responses to individual climate forcers: A PDRMIP multimodel study. *Geophys. Res. Lett.*, **43**, 2782–2791, https://doi.org/10.1002/2016GL068064.
- Sen, P. K., 1968: Estimates of the regression coefficient based on Kendall's tau. J. Amer. Stat. Assoc., 63, 1379–1389, https:// doi.org/10.1080/01621459.1968.10480934.
- Shaw, T. A., and A. Voigt, 2015: Tug of war on summertime circulation between radiative forcing and sea surface warming. *Nat. Geosci.*, **8**, 560–566, https://doi.org/10.1038/ngeo2449.
- Singh, D., 2016: South Asian monsoon: Tug of war on rainfall changes. *Nat. Climate Change*, 6, 20–22, https://doi.org/ 10.1038/nclimate2901.
- Song, F., T. Zhou, and Y. Qian, 2014: Responses of East Asian summer monsoon to natural and anthropogenic forcings in the

- 17 latest CMIP5 models. *Geophys. Res. Lett.*, **41**, 596–603, https://doi.org/10.1002/2013GL058705.
- —, L. R. Leung, J. Lu, and L. Dong, 2018a: Seasonally dependent responses of subtropical highs and tropical rainfall to anthropogenic warming. *Nat. Climate Change*, 8, 787–792, https://doi.org/10.1038/s41558-018-0244-4.
- —, —, and —, 2018b: Future changes in seasonality of the North Pacific and North Atlantic subtropical highs. *Geophys. Res. Lett.*, **45**, 11 959–11 968, https://doi.org/10.1029/2018GL079940.
- Tan, P.-H., C. Chou, and J.-Y. Tu, 2008: Mechanisms of global warming impacts on robustness of tropical precipitation asymmetry. J. Climate, 21, 5585–5602, https://doi.org/10.1175/ 2008JCLI2154.1.
- Taylor, K. E., R. J. Stouffer, and G. A. Meehl, 2012: An overview of CMIP5 and the experiment design. *Bull. Amer. Meteor. Soc.*, 93, 485–498, https://doi.org/10.1175/BAMS-D-11-00094.1.
- Wang, H., S.-P. Xie, and Q. Liu, 2016a: Comparison of climate response to anthropogenic aerosol versus greenhouse gas forcing: Distinct patterns. *J. Climate*, 29, 5175–5188, https:// doi.org/10.1175/JCLI-D-16-0106.1.
- ——, H. Tokinaga, Q. Liu, and Y. Kosaka, 2016b: Detecting cross-equatorial wind change as a fingerprint of climate response to anthropogenic aerosol forcing. *Geophys. Res. Lett.*, 43, 3444–3450, https://doi.org/10.1002/2016GL068521.
- Wang, L., Q. Liu, L. Xu, and S.-P. Xie, 2013: Response of mode water and subtropical countercurrent to greenhouse gas and aerosol forcing in the North Pacific. J. Ocean Univ. China, 12, 191–200, https://doi.org/10.1007/s11802-013-2193-x.

- Wang, Z., L. Lin, M. Yang, Y. Xu, and J. Li, 2017: Disentangling fast and slow responses of the East Asian summer monsoon to reflecting and absorbing aerosol forcings. *Atmos. Chem. Phys.*, 17, 11 075–11 088, https://doi.org/10.5194/acp-17-11075-2017.
- Xie, S.-P., C. Deser, G. A. Vecchi, J. Ma, H. Teng, and A. T. Wittenberg, 2010: Global warming pattern formation: Sea surface temperature and rainfall. *J. Climate*, 23, 966–986, https://doi.org/10.1175/2009JCLI3329.1.
- ——, B. Lu, and B. Xiang, 2013: Similar spatial patterns of climate responses to aerosol and greenhouse gas changes. *Nat. Geo-sci.*, 6, 828–832, https://doi.org/10.1038/ngeo1931.
- —, and Coauthors, 2015: Towards predictive understanding of regional climate change. *Nat. Climate Change*, 5, 921–930, https://doi.org/10.1038/nclimate2689.
- Xu, Y., and S.-P. Xie, 2015: Ocean mediation of tropospheric response to reflecting and absorbing aerosols. *Atmos. Chem. Phys.*, 15, 5827–5833, https://doi.org/10.5194/acp-15-5827-2015.
- Yang, M., S. G. Howell, J. Zhuang, and B. J. Huebert, 2009: Attribution of aerosol light absorption to black carbon, brown carbon, and dust in China—Interpretations of atmospheric measurements during EAST-AIRE. Atmos. Chem. Phys., 9, 2035–2050, https://doi.org/10.5194/acp-9-2035-2009.
- Zhai, P., X. Zhang, H. Wan, and X. Pan, 2005: Trends in total precipitation and frequency of daily precipitation extremes over China. *J. Climate*, **18**, 1096–1108, https://doi.org/10.1175/JCLI-3318.1.
- Zhou, T., and Coauthors, 2009: Why the western Pacific subtropical high has extended westward since the late 1970s. *J. Climate*, **22**, 2199–2215, https://doi.org/10.1175/2008JCLI2527.1.